Reproducible Fog Simulation for Testing Automotive Surround Sensors

Sinan Hasirlioglu, Igor Doric, Alexander Kamann and Andreas Riener
Center of Automotive Research on Integrated Safety Systems and Measurement Area (CARISSMA),
Technische Hochschule Ingolstadt, Germany, 85049
Email: {sinan.hasirlioglu, igor.doric, alexander.kamann, andreas.riener}@thi.de

***Abstract*—Intelligent vehicles use surround sensors such as radar, lidar and camera to perceive their local environment. The generated information are processed by a control unit to identify critical traffic situations such as rear-end collisions and trigger reversible or irreversible safety systems. Incorrect measurements can result in accidents with fatal consequences. Therefore, high reliability and accuracy is a mandatory requirement. The performance of surround sensors depend on the ambient atmosphere and weather conditions. It is known that fog has a negative influence on wave propagation especially in the visible range. Hence, surround sensors must be tested under realistic conditions. To cope with this problem, this paper presents a novel setup together with a test methodology to investigate the influence of fog on automotive radar, lidar and camera sensors. Based on static indoor tests, we have shown that the measurements are consistent with literature and enable reproducible testing.**

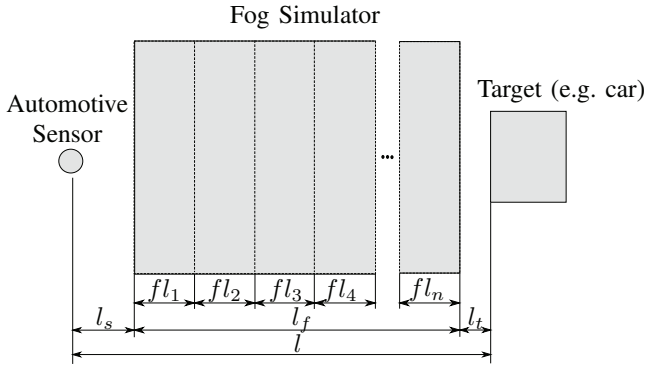

Fig. 1. Principle of the test methodology for testing the influence of fog on automotive surround sensors.

I. Introduction

Inadequate visibility due to environmental factors are one of the main risk factors for road traffic injuries [1]. For example, in foggy conditions, the human detection performance of imminent collisions declines with increasing velocity of the ego vehicle. Compared to younger drivers, older drivers have a decreased sensitivity in dense fog [2]. In the presence of fog, light is scattered by the small particles in the air which results in reduced contrast, color saturation and a loss of precision in contours and details. These discrepancies increase depending on the distance to the object. The consequence is overestimation of the distance to the object ahead [3].

Automotive manufacturers place a high value on the performance of safety systems. Active safety systems aim to prevent accidents and reduce the risk of injury to vehicle occupants and vulnerable road users by the detection of the environment using surround sensors. Typical automotive surround sensors are radar, lidar and camera sensors [4].

Field operational tests have proven to be a good test method for testing active safety systems under realistic settings [5]. Unfortunately, these tests are not reproducible and do not include all environmental conditions. One possible solution is to conduct deterministic, controllable and reproducible indoor tests. The authors in [6] presented a methodology for testing automotive surround sensors on rain influence and have shown that reproducible replication of adverse weather conditions decreases the test effort and supports test driven development at an early development stage. Rain produces much less attenuation in the visible and near infrared spectrum than fog.

Fog consists of microscopic water droplets at ground level with diameter less than $100\,\mu\mathrm{m}$ and can be characterized by visibility, particle size distribution and concentration. Visibility is defined as the distance to an object where a light beam with the wavelength $\lambda = 550\,\mathrm{nm}$ is attenuated to 2% of its origin power [7]. Fog is present when the visibility of the scene decreases to less than 1 km and the relative humidity of the ambient atmosphere reaches saturation level [8]. Some fog banks are more dense than others, because droplets can absorb more water and grow in size. Scattering depends on the wavelength of the electromagnetic wave and the size distribution of droplets [9]. If the particle size is small compared to the wavelength, the amount of light scattered forward and backward is nearly equal (Rayleigh scattering). If the particle size is equal or larger than the wavelength, forward scattering predominates (Mie scattering). Larger particles scatter according to laws of geometric optics [10].

This paper is organized as follows. Section II gives an overview about the related work of fog influence on surround sensors. The test methodology for testing the fog influence and the developed indoor fog simulator are presented in section III. Section IV discusses the test results for standard automotive radar, lidar and camera sensors. Section V summarizes the results and the scientific contribution of this paper.

978-1-5090-5932-4/17/$31.00 ©2017 IEEE

II. Related Work

McKnight and Miles investigated in [11] the impact of reduced visibility on laser based positioning sensors. They replicated atmosphere specific attenuation by the use of a smoke machine, which evaporates glycerol or oil based liquids. Ryde and Hillier presented in [12] a repeatable method for the comparison of lidar and radar sensors under a variation of environmental conditions like dust, rain and mist. The rain and mist replication is realized by a sprinkler system and can be set to variable conditions using a regulator. Low flow rates for larger particles and high flow rates for misty conditions. The concept was not able to generate foggy conditions, because the drop's size was too large. Grabner and Kvicera investigated in [13] the wavelength dependence of the extinction coefficient in fog and haze using Mie's theory in the wavelength interval between $0.3\,\mu\text{m} < \lambda < 2\,\mu\text{m}$ for visibilities lower than 10 km. The influences of fog on optical communication can be found in [14]. The Kruse model predicts the specific attenuation using the local visibility and is given by

$$Attenuation = \frac{3.91}{V}\left(\frac{\lambda}{\lambda_0}\right)^{-q}, (\text{dB/km}) \tag{1}$$

where V is the visibility in km, λ the wavelength in nm, λ_0 the visibility reference wavelength (550 nm) and q the coefficient related to particle size distribution in the atmosphere. q depends on the visibility and can be calculated as follows

$$q = 0.585V^{\frac{1}{3}} \text{ for } V < 6\,\text{km}. \tag{2}$$

Hence, with increasing wavelength λ the atmospheric attenuation decreases.

Kim modified the Kruse model to improve the match to attenuation at low visibilities as seen in [15]. The coefficient q is equal to zero for visibilities lower than 500 m. Al Naboulsi et al. presented in [16] a new approach, where advection fog and radiation fog are modeled separately. Our approach is the generation of fog without glycol or glycerin based fluids or boiling processes to disturb automotive surround sensors in realistic manner.

III. Materials and Methods

The ambient atmosphere provokes scattering and absorption effects to the transmitted electromagnetic wave by small particles of ice, snow or water. For testing the influence of fog on automotive surround sensors, a fog simulator together with a test methodology was developed and validated.

A. Test Methodology

Basis of the test methodology is a fog simulator with the length l_f. Figure 1 shows the principle setup in top view. The fog simulator consists of several switchable fog layers with the length f_n. The layers are areas with replicated fog and are used to disturb the surround sensor. The number of activated fog layers allows to control the level of disturbance. The disturbance on the sensor is increased by incrementing the number of activated fog layers. As soon as the sensor can not distinguish between target and disturbance, the sensor limit and critical operating point is reached. The sensor under test is mounted in front of the simulator at a distance of l_s. The target object is mounted behind the fog simulator at a distance of l_t. The distance between sensor and target is l. The configuration as shown in figure 1 is used to disturb the transmitted electromagnetic waves by enabling absorption and scattering effects. The effect of water covered sensor or target can be added by setting l_s or l_t to zero.

Fig. 2. Fog simulator based on 27 ultrasonic transducer plates per layer.

First, the target is measured by the sensor under test without any influence of fog. Subsequently, the first fog layer fl_1 is activated and the path between sensor and object will be disturbed by small water particles. The measurement of the target is still running. Then, the second fog layer fl_2 is activated. Based on transmission, reflection and absorption the disturbance will increase through the higher quantity of water particles. This procedure is continued incrementally until all layers, including the last layer fl_n, are activated and measured by the sensor under test. Basic principle of our sensor benchmark methodology is that at a specific fog layer the sensor can not distinguish between fog and target. Therefore, the number of fog layers is the assessment criterion.

The test methodology can also be used to validate theoretical models. In previous work [17], we presented a model to predict the sensor behavior of laser scanners under rain influence. The basis is an abstraction to a virtual layer model, whose layer thickness is equal to the sensor resolution. A virtual layer considers physical effects like transmission, reflection and absorption. The sum of all received intensities can be described for a lidar sensor as

$$I_\kappa = I_0 \cdot \sum_{i=1}^{\frac{\kappa-1}{2}} p_i \cdot \varrho^{2i-1} \cdot \tau^{\kappa+1-2i} \tag{3}$$

where I_κ is the received and I_0 the transmitted intensity. τ characterize the transmittance and ϱ the reflectance of one single layer. κ is the number of penetrated layers, which is

the sum of the exponents of τ and ϱ, and p_i the number of occurrence of this path. p_i is calculated by Dyck paths using Catalan and Narayana numbers and enables multiple reflections. The highest intensity, reflected by the target object I_{obj} can be described as

$$I_{obj} = I_0 \cdot \varrho_{obj} \cdot \tau^{2\kappa} \tag{4}$$

where ϱ_{obj} is the reflectivity of the object. Equation 4 describes the received intensity, if the transmitted wave travels straight to the object and returns back without any reflections from disturbance layers. This principle can be adapted to a fog model by changing the properties of ϱ and τ according to drop size distribution and particle size of fog.

B. Test setup

An important characteristic of the developed fog simulator is, that no glycol or glycerin based fluids are vaporized. The replicated fog consists only of clear water without any boiling process to ensure same physical characteristics as real fog regarding scattering and absorption. This is realized by the use of ultrasonic foggers. The basis of this device is a metallic ultrasonic transducer plate. By vibrating at ultrasonic frequency, the water molecules break apart into particular droplets with diameter about 1 µm and are evaporated into the air flow. This results in a cool, thick fog bank. Best performance is reached, if the fogger is located below the water surface. A specially designed buoy holds the ultrasonic fogger between 20 and 35 mm under water.

For testing automotive surround sensors, the transmitted electromagnetic wave is disturbed by the replicated fog bank. For this purpose and to ensure long measurement time, the ultrasonic foggers are placed in a rain barrel. One rain barrel includes 27 transducer plates, which evaporate 15 liters of water per hour and provide the necessary amount of fog for one layer which is presented in the test methodology. The generated fog inside the barrel is transported to the outside through round tubes by the use of an integrated fan.

Figure 2 shows the developed and constructed fog simulator for the test of automotive surround sensors. Four rain barrels are used to generate a 4 m fog bank. For validation of the fog simulator, the visual range measuring device VISIC620 is used. This sensor system measures the visibility, based on the diffusion of light by particles. Figure 3 shows the increasing specific attenuation due to the activation of one fog layer, which can be calculated by

$$A = 10 \log(e) \beta \tag{5}$$

where A is the attenuation in dB/km and β is the extinction coefficient in km^{-1} measured by the VISIC620.

The extinction coefficient increases from 0.33 to more than 900 km^{-1}. This results in a measured visibility of 5.74 m. The visibility is related to the extinction coefficient β by

$$V = -\frac{ln(\epsilon)}{\beta} \tag{6}$$

where ϵ is the threshold of contrast and equal to 0.02 [18].

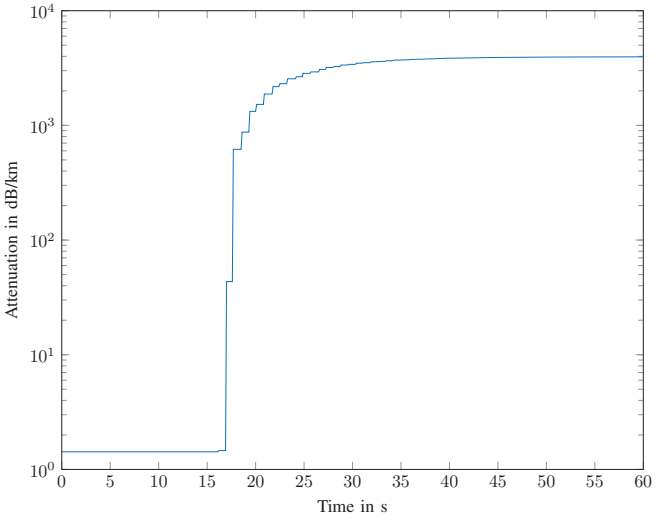

Fig. 3. Measured specific attenuation within each fog layer.

Realistic and reproducible tests can be performed, using the standardized Euro NCAP Vehicle Target (EVT). The solid construction of the EVT is recognizable for current generation of surround sensors and can be used for stationary and dynamic scenarios. More details of the EVT are presented by ADAC in [19]. The following measurements are performed with the configuration $l_s = 2$ m, $l_f = 4$ m, $l_t = 4$ m and $fl = 1$ m.

IV. Fog Influence on Automotive Surround Sensors

A. Radar

Radar (Radio detection and ranging) sensors uses electromagnetic waves in millimeter range to measure the distance, angle and velocity of surrounding objects. They are extensively used for autonomous driving and safety systems, like adaptive cruise control or collision mitigation systems [20]. Therefore, high accuracy and reliability is mandatory.

Environmental influences on radar sensors has been studied before. Brooker et al. presented in [21] a theoretic summary of the performance of radar sensors through clouds of coal dust and water droplets in the mining environment. The conclusion is that the effect of backscatter is almost negligible for radar sensors with a frequency of 77 GHz and 94 GHz and becomes only significant at visibilities less than 4 m with large droplet size. Balal et al. provides in [22] an overview about the fog effects on ultra wide band radars at frequencies higher than 30 GHz. A millimeter wave propagation model is developed to study the dispersive effects caused by atmospheric medium. They found that foggy conditions affect the accuracy of the radar sensor, caused by deviation in frequency and phase of the received signal. Hawkins et al. developed a theoretical approach to compare the abilities of pulse radar to detect targets in rain and fog [23]. In this approach combined effects of attenuation and backscattering are described. Mori et al. described in [24] a method to determine fog density using in-vehicle radar and camera sensor. Further, a classifier is

used to classify fog into three classes. Experimental results showed a recognition rate of 84% by comparison with human observations.

The setup for testing automotive radar sensors was built as shown in figure 1. A state of the art automotive long range radar with a frequency of 77 GHz was used for the following measurements. For each measurement with a specific number of fog layers a measurement series containing 200 single measurements is used. Measurement series were recorded under incremental activation of fog layers. The evaluation is based on the radar cross section (RCS) of tracked objects.

RCS is the measure of an obstacles capability to reflect signals in the radar receivers direction. The RCS of complex targets such as vehicles and vulnerable road users is depending on the size, shape, orientation and material, which has influence on the maximum detectable range, target detectability and tracking stability. In [20] the radar cross section of different targets like sedan, small van, bicycle, manned bicycle and pedestrian are analyzed. Therefore, the identification based on RCS values of various targets might be enabled. The human RCS value is approximately -8 dBsm and rear of vehicles RCS is approximately 7-12 dBsm [25].

The RCS of surrounding targets can be calculated by

$$\sigma = \frac{(4\pi)^3 \cdot R^4}{P_t \cdot G^2 \cdot \lambda^2} \cdot P_r \tag{7}$$

where σ is the obstacles RCS value, P_t the transmitted and P_r the received power, R the distance between sensor and target, G the antenna gain and λ the transmitting wavelength [20].

Figure 4 shows the RCS values for measurement series with increasing number of fog layers in a box plot. The first box shows the mean RCS value without the influence of fog, which is 14.97 dBsm. This value is higher than the expected value, which might be caused by multiple indoor reflection. Activating the first and second fog layer has almost no effect.

The RCS median value is almost constant for each measurement step. Small variations are consequences of the sensor uncertainty. The first three fog layers show almost no effect on the used radar sensor. Four activated fog layers cause some outliers, which shows that scattering effects are present. At higher number of activated fog layers a more drastic disturbance can be expected. However, it is shown that radar is quite resistant against fog influence in the presented test setup. Algorithms using the RCS value for object classification are stable in foggy conditions. Compared to rain influence, the attenuation is much less under fog influence and can be also seen in [6] and [26].

The complex refractive index is an usual measure of an electromagnetic wave traveling through a medium, e.g. water. The imaginary part implies the absorption of a medium. For long range radar sensors operating at a frequency of 77 GHz both, the real and imaginary part of the refractive index are relatively high, leading to a higher attenuation than lidar sensors [27]. This means, that effects like water covered sensors adversely affect the wave propagation. Compared to rain or water covered sensors, foggy conditions are not critical

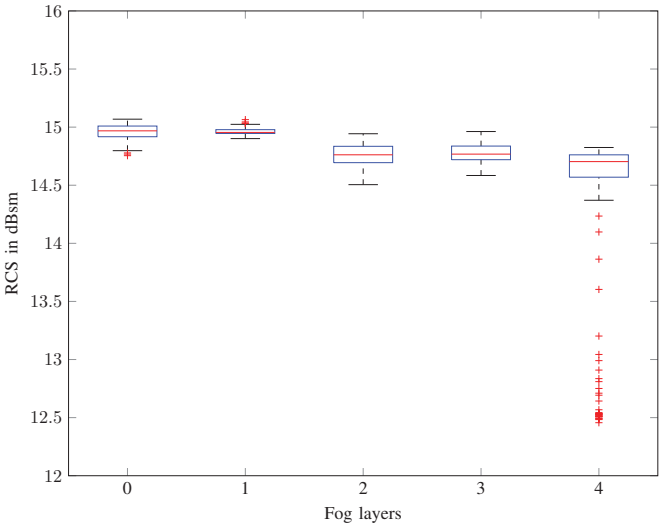

Fig. 4. RCS values of target object with increasing number of fog layers.

for the performance of automotive radar. The presented test methodology can be used for the test of automotive radar sensors. However, low attenuation does not imply, that test in foggy conditions are unnecessary. Especially the robustness of new radar sensors or the functionality of novel algorithms must be validated.

B. Lidar

The first lidar (light detection and ranging) application was used in meteorology for cloud measurements. Variations in signal intensity depending on the distance provide information about the atmospheric properties. Fiocco and Smullin used 1963 a ruby laser to detect reflections from the atmosphere at heights up to 140 km [28]. Nowadays, in the field of intelligent vehicles, lidar sensors are used as an environment detection sensor for safety functions or autonomous driving. The time of flight principle is used to determine the distance to an object. A short duration laser pulse is emitted from the laser light source, reflected by the target and captured by the receiver.

In [29] the impact of environmental water on lidar sensors has been analyzed. They showed that 0.9 µm wavelength is comparably weather resistant and recommended it for applications in environments with changing weather conditions. Rasshofer et al. provide in [30] an overview on physical principles for laser disturbance in rainy and foggy situations, where Mie's theory is used for the calculation of extinction and the backscattering efficiency. For foggy environments, they recorded laser signals in real fog scenarios and simulated it in the laboratory using an electro optical laser target simulator system. Zhu et al. published in [31] the idea of weather detection using camera and lidar sensors. They presented a system to compare measured lidar data points with a stored data set for the estimation of the weather condition. Dannheim et al. described in [32] a combination of camera and lidar for the estimation of weather conditions in front of the moving ego vehicle using various neural algorithms.

The Hokuyo UTM-30LX-EW laser range finder (λ=905 nm) is used for the following measurements [33]. The two dimensional scanning sensor measures distances up to 30 m with a resolution of 0.25° and a scan frequency of 40 Hz. The results presented below show the influence of fog on lidar sensors.

Figure 5 illustrates single scans of the laser range finder. The scan on the far left is recorded without any fog influence. The measurements on the right are recorded under stepwise increasing fog layers. The scan on the far right is made with four activated fog layers. The gray bar on top indicates the region of the EVT. The static points on the left are reflected by the wall and the used rain barrels which can also be seen in figure 2 and are marked by the circles in figure 5. The sensor under test is centered at the bottom of each plot.

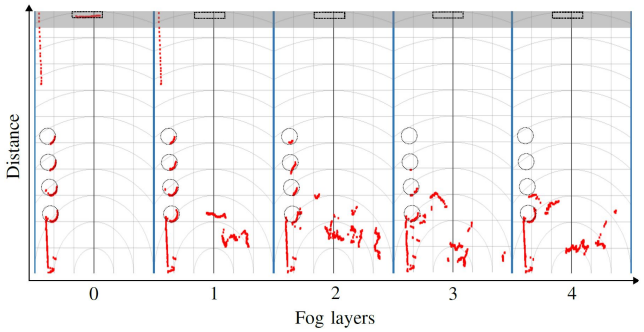

Fig. 5. Measurements with lidar sensor (single scan per plot). After activating one layer, the sensor measures only the fog and cannot detect any reflections from the target object.

The target is measured correctly, if no measurement points between sensor and target are present. Activating fog layers lead to reflections from water particles of the fog bank. Even after activating one layer, all lidar pulses are reflected by fog. The sensor cannot detect any reflections from the EVT.

The Hokuyo sensor uses the multi echo technology for the detection of up to three echos in one direction. However, due to the high density of the fog bank, nearly no laser light reaches the target object. Therefore, the activation of more than one fog layer has almost no further effect.

Figure 6 shows the relative intensity of points in one direction, which are reflected from the EVT and received by the laser scanner depending on the number of activated fog layers. Box plots with outliers and distribution indicate clearly the strong decrease of intensity. Each box plot contains 40 consecutive points of the same angle. Without the influence of fog, the mean relative intensity is around 540, which is the maximum achievable value for this test configuration. With the activation of the first layer the median intensity of the EVT drops by 100%. Due to the dynamic of fog bank, some regions are denser than others, which results in a few outliers. After activating the second fog layer, the fog bank is dense enough, so the complete signal is absorbed and scattered. Since no signal is received from the EVT the lidar sensor has reached its limit in this test setup.

Figure 5 also shows that the measured points in fog are shifted from their origin position. Hence, the distance between

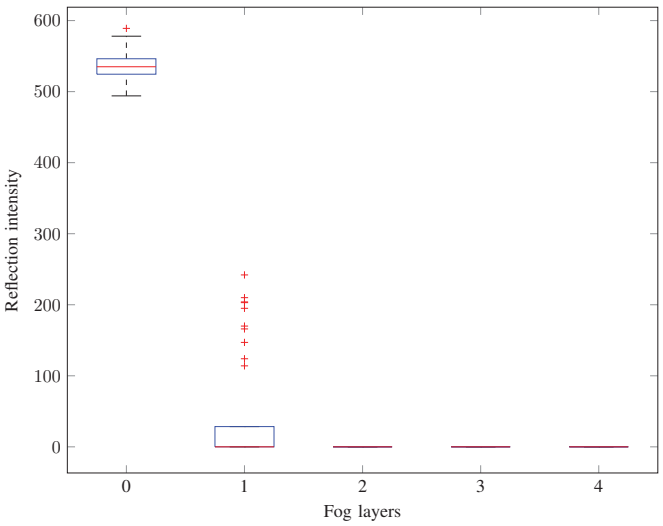

Fig. 6. Reflection intensity of the target object depending on the number of activated fog layers (40 scans per box plot).

two neighboring points increases. In a segmentation process, e.g. adaptive breakpoint detector, the distance between two points determines whether the point belongs to the same segment or not [34]. In this case, the target will be classified as several objects and false positive objects will be generated.

The presented test methodology can be used to disturb the perception of the environment of lidar sensors. For benchmarking sensors, the same test methodology can be applied to further lidar sensors. The sensor with more intense reflections from the EVT depending on the activated fog layers can be rated as more fog resistant than another.

C. Camera

Cameras are one of the most intensive researched sensors in the field of automotive safety. The most important features for image processing are edges and corners. Regarding fog influence, many existing models and detection algorithms are based on the Koschmieder's law which describes the effect of fog on atmospheric visibility. The apparent luminance $L(u, v)$ can be calculated as

$$L(u,v) = L_0(u,v)e^{-\beta d(u,v)} + L_s(1 - e^{-\beta d(u,v)}) \quad (8)$$

where $L_0(u, v)$ is the intrinsic luminance, β the extinction coefficient, $d(u, v)$ is the object distance of pixel position (u, v) and L_s the luminance of the sky. The extinction coefficient β of fog is related to the meteorological visibility d_m defined by the International Commission on Illumination (CIE) and is described as [35]

$$d_m = -\frac{ln(0.05)}{\beta}. \quad (9)$$

Tarel et al. published in [36] an overview about the state of the art visibility enhancement algorithms, discussing their advantages and limits. For the evaluation, synthetic images with different types of synthetic fog are used. Narasimhan

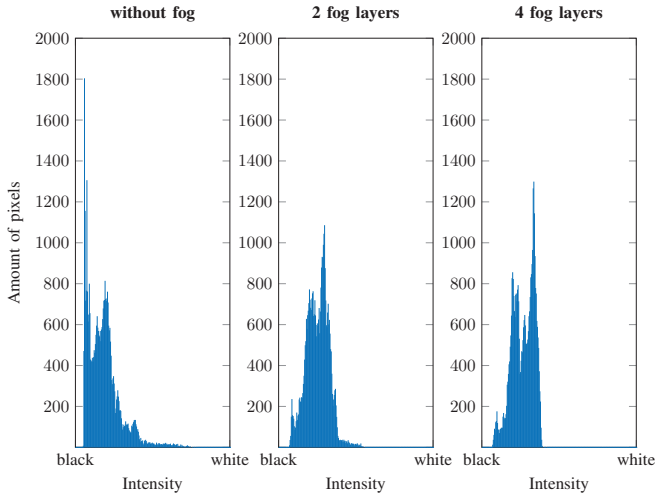

Fig. 7. Histograms of standard automotive camera images of the EVT without fog influence, with two activated fog layers and four activated fog layers.

and Nayar published in [37] a physical model that specifies the appearance of extreme weather conditions like fog. Further, they presented an algorithm for restoring the loss in contrast.

Figure 8 shows a series of images of the EVT recorded by a standard automotive camera sensor. During the test procedure, images are recorded continuously. The region of interest (area of the EVT) of the images are extracted and converted into gray scale. The image far left is taken without any fog influence. The image far right is taken with four activated fog layers.

It is clear that with increasing number of activated fog layers, the disturbance increases. The influence of small water particles in the air is most visible on dark background. The fog influence is less visible on bright background. It can be clearly seen that fog changes the pixel intensity to a shade of gray.

The edge detection becomes more challenging, due to the loss in contrast. A more representative evaluation can be obtained by generating the histograms of the images without fog, with two activated layers and with four activated layers as shown in figure 7. The horizontal axis of the histogram represents the gray level intensities. The vertical axis represents the amount of pixels in the corresponding intensity. In the histogram without fog can be seen, that most of the pixels are predominantly on the left side, which represents the dark area. In the histogram with two activated fog layers, the mean and maximum value are shifted to the right. Four activated fog layers lead to further shift of the mean and maximum value to the right. It can also be seen that the activation of fog layers leads to decreased tonal range. The mean intensity of the histogram without fog is 46, while the mean intensity of the histogram with two activated fog layers is 64, reaching a maximum of 68 with four activated fog layers. A shift to the right corresponds to a brighter image and a smaller tonal range corresponds to less contrast.

Brightening is based on the reflection of light from small water particles of the generated fog. Specular and internal reflections additionally increase the brightness. Consequently, the droplets tends to be brighter than their background [38]. The problem of restoring the contrast of atmospherically degraded images are adressed in [37].

Increased number of activated fog layers and consequently lower contrast in images makes it more complex to detect objects like vulnerable road users or vehicles, due to the reduced amount of relevant features like edges and corners. In the field of automotive safety, a minor error can lead to major injuries. Hence, tests under various weather conditions are mandatory. The proposed test methodology can be used to validate and improve camera based detection algorithms under various and reproducible fog influence.

V. Summary and Future Work

This paper presents a test methodology for standard automotive surround sensors under foggy conditions. The methodology is based on the disturbance of electromagnetic waves by a developed indoor fog simulator consisting of individual switchable fog layers. No glycol or glycerin based fluids are vaporized for fog generation, to ensure real scattering and absorption properties. The characteristic of the generated fog was measured using a standard visual range measuring device. The sensor disturbance is increased by incrementing the number of fog layers. The sensor limit is reached, when the object reflections and reflections by the disturbing fog can not be differed by the sensor anymore. This principle can be used for the quantification of fog robustness for different sensor systems and was demonstrated in this paper using standard automotive radar, lidar and camera sensors. Furthermore, the presented methodology can be used for benchmarking the robustness of different sensor systems, where the number of activated fog layers serves as assessment criterion.

Fig. 8. Series of images of the target object under incremental increasing fog layers; far left: no fog influence, far right: four activated fog layers.

In the presented test setup, radar sensors show to be robust regarding fog influence, while lidar sensors are strongly affected and reach their critical operation point. For camera systems, the increased number of activated fog layers lead to lower contrast and hence to a reduced amount of edges and corners, which are relevant features for object detection.

In future work, the test setup will be expanded in length. Furthermore, a variation of different fog intensities will be integrated in the presented simulator. Especially, in the context of automated driving, the effects of various weather conditions must be considered and handled in order to ensure required safety and reliability in all weather conditions. The combination of real driving tests with reproducible indoor tests under defined weather conditions can be the key to handle the huge amount of test effort, which is necessary to test complex systems like autonomous driving functions.

REFERENCES

[1] M. Peden, R. Scurfield, D. Sleet, D. Mohan, A. Hyder, E. Jaravan, and C. Mathers, Eds., *World report on road traffic injury prevention*. Geneva: World Health Organization, 2004.

[2] R. Ni, Z. Bian, A. Guindon, and G. J. Andersen, "Aging and the detection of imminent collisions under simulated fog conditions," *Accident Analysis and Prevention*, vol. 49, pp. 525–531, 2012.

[3] V. Cavallo, M. Colomb, and J. Doré, "Distance perception of vehicle rear lights in fog," *Human Factors: The Journal of the Human Factors and Ergonomics Society*, vol. 43, no. 3, pp. 442–451, 2001.

[4] W. J. Fleming, "New automotive sensors—a review," *IEEE Sensors Journal*, vol. 8, no. 11, pp. 1900–1921, 2008.

[5] M. Benmimoun, A. Pütz, A. Zlocki, and L. Eckstein, "eurofot: Field operational test and impact assessment of advanced driver assistance systems: Final results," in *Proceedings of the FISITA 2012 World Automotive Congress*, ser. Lecture Notes in Electrical Engineering. Berlin, Heidelberg: Springer Berlin Heidelberg, 2013, vol. 197, pp. 537–547.

[6] S. Hasirlioglu, A. Kamann, I. Doric, and T. Brandmeier, "Test methodology for rain influence on automotive surround sensors," in *2016 IEEE 19th International Conference on Intelligent Transportation Systems (ITSC)*, pp. 2242–2247.

[7] F. Nadeem, T. Javornik, E. Leitgeb, V. Kvicera, and G. Kandus, "Continental fog attenuation empirical relationship from measured visibility data," *Radioengineering*, 2010.

[8] F. Nadeem and E. Leitgeb, "Dense maritime fog attenuation prediction from measured visibility data," *Radioengineering*, vol. 19, no. 2, pp. 223–227, 2010.

[9] E. Dumont and V. Cavallo, "Extended photometric model of fog effects on road vision," *Transportation Research Record: Journal of the Transportation Research Board*, vol. 1862, pp. 77–81, 2004.

[10] H. C. Hulst, *Light Scattering by Small Particles*, ser. Dover Books on Physics. Newburyport: Dover Publications, 2012. [Online]. Available: http://gbv.eblib.com/patron/FullRecord.aspx?p=1894337

[11] D. McKnight and R. Miles, "Impact of reduced visibility conditions on laser-based dp sensors," 2014.

[12] J. Ryde and N. Hillier, "Performance of laser and radar ranging devices in adverse environmental conditions," *Journal of Field Robotics*, vol. 26, no. 9, pp. 712–727, 2009.

[13] M. Grabner and V. Kvicera, "The wavelength dependent model of extinction in fog and haze for free space optical communication," *Optics express*, vol. 19, no. 4, pp. 3379–3386, 2011.

[14] P. W. Kruse, L. D. McGlauchlin, and R. B. McQuistan, *Elements of infrared technology: Generation, transmission and detection*, 1962.

[15] I. I. Kim, B. McArthur, and E. J. Korevaar, "Comparison of laser beam propagation at 785 nm and 1550 nm in fog and haze for optical wireless communications," *Proc. SPIE*, vol. 4214, 2001. [Online]. Available: http://dx.doi.org/10.1117/12.417512

[16] M. Al Naboulsi, H. Sizun, and Fornel, Fre de rique de, "Fog attenuation prediction for optical and infrared waves," *Optical Engineering*, vol. 43, no. 2, pp. 319–329, 2004. [Online]. Available: http://dx.doi.org/10.1117/1.1637611

[17] S. Hasirlioglu, I. Doric, C. Lauerer, and T. Brandmeier, "Modeling and simulation of rain for the test of automotive sensor systems," in *2016 IEEE Intelligent Vehicles Symposium (IV)*, pp. 286–291.

[18] B. A. Kunkel, "Parameterization of droplet terminal velocity and extinction coefficient in fog models," *Journal of Climate and Applied Meteorology*, vol. 23, no. 1, pp. 34–41, 1984.

[19] V. Sandner, "Development of a test target for aeb systems," *23rd International Technical Conference on the Enhanced Safety of Vehicles (ESV): Research Collaboration to Benefit Safety of All Road Users*, 2013.

[20] I. Matsunami, R. Nakamura, and A. Kajiwara, "Rcs measurements for vehicles and pedestrian at 26 and 79ghz," in *Signal Processing and Communication Systems (ICSPCS), 2012 6th International Conference on*, 2012, pp. 1–4.

[21] G. Brooker, R. Hennessey, C. Lobsey, M. Bishop, and E. Widzyk-Capehart, "Seeing through dust and water vapor: Millimeter wave radar sensors for mining applications," *Journal of Field Robotics*, vol. 24, no. 7, pp. 527–557, 2007.

[22] N. Balal, G. A. Pinhasi, and Y. Pinhasi, "Atmospheric and fog effects on ultra-wide band radar operating at extremely high frequencies," *Sensors (Basel, Switzerland)*, vol. 16, no. 5, 2016.

[23] H. E. Hawkins and O. La Plant, "Radar performance degradation in fog and rain," *IRE Transactions on Aeronautical and Navigational Electronics*, vol. ANE-6, no. 1, pp. 26–30, 1959.

[24] K. Mori, T. Takahashi, I. Ide, H. Murase, T. Miyahara, and Y. Tamatsu, "Recognition of foggy conditions by in-vehicle camera and millimeter wave radar," in *2007 IEEE Intelligent Vehicles Symposium*, 2007, pp. 87–92.

[25] N. Yamada, Y. Tanaka, and K. Nishikawa, "Radar cross section for pedestrian in 76ghz band," in *2005 European Microwave Conference*, vol. 2, 2005.

[26] A. A. Hassen, *Indicators for the signal degradation and optimization of automotive radar sensors under adverse weather conditions: Zugl.: Darmstadt, Techn. Univ., Diss., 2006*, ser. Berichte aus der Hochfrequenztechnik. Aachen: Shaker, 2007.

[27] D. J. Segelstein, *The complex refractive index of water*, 1981.

[28] G. Fiocco and L. D. Smullin, "Detection of scattering layers in the upper atmosphere (60-140 km) by optical radar," *Nature*, vol. 199, no. 4900, pp. 1275–1276, 1963.

[29] J. Wojtanowski, M. Zygmunt, M. Kaszczuk, Z. Mierczyk, and M. Muzal, "Comparison of 905 nm and 1550 nm semiconductor laser rangefinders' performance deterioration due to adverse environmental conditions," *Opto-Electronics Review*, vol. 22, no. 3, 2014.

[30] R. H. Rasshofer, M. Spies, and H. Spies, "Influences of weather phenomena on automotive laser radar systems," *Advances in Radio Science*, vol. 9, pp. 49–60, 2011.

[31] J. Zhu, D. Dolgov, and D. Ferguson, "Methods and systems for detecting weather conditions including fog using vehicle onboard sensors," 2015. [Online]. Available: https://www.google.com/patents/US8983705

[32] C. Dannheim, C. Icking, M. Mader, and P. Sallis, "Weather detection in vehicles by means of camera and lidar systems," in *Computational Intelligence, Communication Systems and Networks (CICSyN), 2014 Sixth International Conference on*, 2014, pp. 186–191.

[33] L. Hokuyo Automatic Co., "Scanning laser range finder utm-30lx-ew specification," 2012.

[34] G. A. Borges and M.-J. Aldon, "Line extraction in 2d range images for mobile robotics," *J. Intell. Robotics Syst.*, vol. 40, no. 3, pp. 267–297, 2004.

[35] N. Hautiére, J.-P. Tarel, J. Lavenant, and D. Aubert, "Automatic fog detection and estimation of visibility distance through use of an onboard camera," *Machine Vision and Applications*, vol. 17, no. 1, pp. 8–20, 2006.

[36] J.-P. Tarel, N. Hautiere, L. Caraffa, A. Cord, H. Halmaoui, and D. Gruyer, "Vision enhancement in homogeneous and heterogeneous fog," *IEEE Intelligent Transportation Systems Magazine*, vol. 4, no. 2, pp. 6–20, 2012.

[37] S. G. Narasimhan and S. K. Nayar, "Contrast restoration of weather degraded images," *IEEE Transactions on Pattern Analysis and Machine Intelligence*, vol. 25, no. 6, pp. 713–724, 2003.

[38] K. Garg and S. K. Nayar, "Vision and rain," *International Journal of Computer Vision*, vol. 75, no. 1, pp. 3–27, 2007.